Anal. Chem. **2002,** *74,* 5001−5008

Electroanalysis of Metabolic Flux from Single Cells in Simple Picoliter-Volume Microsystems

Tomoyuki Yasukawa,*,†,‡ Andrew Glidle,† Jonathan M. Cooper,† and Tomokazu Matsue*,‡

Bioelectronics Research Centre, Department of Electronics & Electrical Engineering, The Rankine Building, Oakfield Avenue, University of Glasgow, Glasgow, G12 8QQ, U.K., and Department of Biomolecular Engineering, Graduate School of Engineering, Tohoku University, Aramaki07, Aoba, Sendai 980-8579, Japan

A picoliter-volume electrochemical analytical chamber has been developed for detecting the metabolic flux resulting from the stress responses of a single plant cell. Electrochemical cells, with volumes as small as 100 pL, were fabricated by controlled electrochemical dissolution of a gold wire sealed in glass (the back-etching of the metal realizing an ultralow-volume titer chamber). In the first instance, the electrode contained within the chamber was characterized by the microinjection of standard aliquots of either ascorbic acid or hydrogen peroxide. In all cases, experimental currents obtained correlated well with theoretical calculations. Subsequently, single plant cells were micromanipulated into the chambers and were exposed to amounts of the detergent SDS (which permeabilized the cell membrane and released the intracellular contents). The flux of metabolite released from a single cell was estimated by using electrochemical-linked assays based upon the enzymes catalase, ascorbate oxidase, and horseradish peroxidase (in each case), in the presence of a mediator. In so doing, we investigated the activity of the cellular protection mechanisms through the determination of peroxides, while the individual cell was "stressed". The technique was found to provide a reliable and reproducible method for making single-cell measurements, using fabrication procedures that are both simple and do not require photolithographic methods.

Over the last twenty years it has been established that, by using suitably positioned microelectrodes, it is possible to analyze metabolites resulting from cell activity using electroanalytical methods. While the voltage clamp technique has focused on the measurement of ions, amperometric methods have enabled the development of a variety of biological measurements. For example, research on neurotransmitter release from neurons,[1−4] on the oxidative burst from fibroblasts,[5−7] on cardiomyocyte physiology during simulated ischemia,[8−10] and on both photosynthetic activity[11−15] and respiration[16−20] have all previously been reported either at the single-cell level or using multicellular preparations, either in vivo or in vitro.

In general, two experimental approaches have been used when amperometric measurements were performed on biological cells. These involve either the production of fiber-type microelectrodes or the fabrication of planar or three-dimensional (3-D) devices using methods adapted from the microelectronic industry.[21] This latter technology is remarkably versatile and is also adaptable to applications in a variety of analytical areas including microelectrochemistry,[22−27] microreactor design,[28−30] and combinatorial syn-

* Corresponding author. Tel: +44−141-330-5764. Fax: +44−141-330-6010. E-mail: yasu@elec.gla.ac.uk.

† University of Glasgow.

‡ Tohoku University.

(1) Baur, J. E.; Kristensen, E. W.; May, L. J.; Wiedemann, D. J.; Wightman, R. M. *Anal. Chem.* **1988**, *60*, 1268−1272.

(2) Wightman, R. M.; Hochstetler, S.; Michael, D.; Travis, E. *Chem. Commun. Interface* **1996**, *5*, 22−26.

(3) Bunin, M. A.; Wightman, R. M. *J. Neurosci.* **1998**, *18*, 4854−4860.

(4) Wightman, R. M.; Jankowski, J. A.; Kennedy, R. T.; Kawagoe, K. T.; Schroeder, T. J.; Leszczyszyn, D. J.; Near, J. A.; Diliberto, E. J.; Viveros, O. H. *Proc. Natl. Acad. Sci. U.S.A.* **1991**, *88*, 10754−10758.

(5) Arbault, S.; Pantano, P.; Jankowski, J. A.; Vuillaume, M.; Amatore, C. *Anal. Chem.* **1995**, *67*, 3382−3390.

(6) Amatore, C.; Arbault, S.; Bruce, D.; Oliveira, P.; Erard, M.; Vuillaume, M. *Faraday Discuss.* **2000**, *116*, 319−333.

(7) Amatore, C.; Arbault, S.; Bruce, D.; Oliveira, P.; Erard, M.; Vuillaume, M. *Chem. Eur. J.* **2001**, *7*, 4171−4179.

(8) Ringel, F.; Schmid-Elsaesser, R. *Expert Opin. Ther. Pat.* **2001**, *11*, 987−997.

(9) Jordan, S.; Mitchell, J. A.; Quinlan, G. J.; Goldstraw, P.; Evans, T. W. *Eur. Respir. J.* **2000**, *15*, 790−799.

(10) Taylor, D. L.; Edwards, A. D.; Mehmet, H. *Brain Pathol.* **1999**, *9*, 93−117.

(11) Matsue, T.; Koike, S.; Abe, T.; Itabashi, T.; Uchida, I. *Biochim. Biophys. Acta* **1992**, *1101*, 69−72.

(12) Matsue, T.; Koike, S.; Uchida, I. *Biochem. Biophys. Res. Commun.* **1993**, *197*, 1283−1287.

(13) Yasukawa, T.; Uchida, I.; Matsue, T. *Biophys. J.* **1999**, *76*, 1129−1135.

(14) Yasukawa, T.; Uchida, I.; Matsue, T. *Denki Kagaku* **1998**, *66*, 660−661.

(15) Yasukawa, T.; Kaya, T.; Matsue, T. *Chem. Lett.* **1999**, 975−976.

(16) Chen, T. K.; Lau, Y. Y.; Wong, D. K. Y.; Ewing, A. G. *Anal. Chem.* **1992**, *64*, 1264−1268.

(17) Lau, Y. Y.; Abe, T.; Ewing, A. G. *Anal. Chem.* **1992**, *64*, 1702−1705.

(18) Abe, T.; Lau, Y. Y.; Ewing, A. G. *J. Am. Chem. Soc.* **1991**, *113*, 7421−7423.

(19) Jung, S. K.; Gorski, W.; Aspinwall, C. A.; Kauri, L. M.; Kennedy, R. T. *Anal. Chem.* **1999**, *71*, 3642−3649.

(20) Yasukawa, T.; Kondo, Y.; Uchida, I.; Matsue, T. *Chem. Lett.* **1998**, 767−768.

(21) Moreau, W. M. *Semiconductor Lithography: Principles and Materials*; Plenum: New York, 1988.

(22) Bratten, C. D. T.; Cobbold, P. H.; Cooper, J. M. *Anal. Chem.* **1997**, *69*, 253−258.

(23) Bratten, C. D. T.; Cobbold, P. H.; Cooper, J. M. *Anal. Chem.* **1998**, *70*, 1164−1170.

(24) Clark, R. A.; Hietpas, P. B.; Ewing, A. G. *Anal. Chem.* **1997**, *69*, 259−263.

(25) Clark, R. A.; Ewing, A. G. *Anal. Chem.* **1998**, *70*, 1119−1125.

(26) Crofcheck, C. L.; Grosvenor, A. L.; Anderson, K. W.; Lumpp, J. K.; Scott, D. L.; Daunert, S. *Anal. Chem.* **1997**, *69*, 4768−4772.

(27) Ball, J. C.; Scott, D. L.; Lumpp, J. K.; Daunert, S.; Wang, J.; Bachas, L. G. *Anal. Chem.* **2000**, *72*, 497−501.

(28) Song, M. I.; Iwata, K.; Yamada, M.; Yokoyama, K.; Takeuchi, T.; Tamiya, E.; Karube, I. *Anal. Chem.* **1994**, *66*, 778−781.

10.1021/ac025836u CCC: $22.00
Published on Web 08/24/2002

thesis.[31] For example, both 2-D (planar)[22,23] and 3-D[32] arrangements of lithographically fabricated recessed electrodes have been incorporated into micromachined electrochemical devices, enabling the study of electroactive species in quiescent, flowing,[33] and confined volumes of solutions.[22,23] In the case of small, confined, volumes of solution, an advantage is that it is possible to detect whole quantities of biological substances produced by single cells, without the loss of metabolites to bulk solution. Cell activity has been measured in picoliter-scale devices micromachined in photoetchable polymers[23] or in nanoliter-sized vials employing two-electrode arrangements. These latter devices were fabricated by combining screen-printing and laser micromachining.[27]

As an alternative strategy, fiber-type microelectrodes also excel as a detector of chemical and biological substances that are generated from single cells. For example, catecholamines released from individual vesicular exocytosis were analyzed with millisecond time resolution and detected at zeptomole levels.[34] However, when positioned fiber-type microelectrodes are used, it is difficult to detect *total* quantities of important biological metabolites within a single cell. In general, interpretation of these measurements requires estimates of the distance of the fiber from the cell, which can be difficult. Notwithstanding this, the use of such microsensor arrangements has proved particularly popular in techniques such as SECM, where the electrode is rastered across the surface, at a fixed height to create a 2-D map of ion flux.[35−37]

In this paper, we propose a new development of a picoliter-scale vial, which includes an integrated (fixed) working microelectrode. This method of fabricating a vial electrode is based on the modification of a composite microelectrode. In brief, devices are fabricated by electrochemical etching of gold embedded in a glass capillary. The resultant cavity, formed in the end of the capillary, is utilized as an ultralow-volume vial into which either single cells or reagents can be readily placed using micromanipulators; see Figure 1. By varying the time of electrochemical etching and the radius of the gold wire, different geometries of electrodes can be readily fabricated with different measurement volumes. To prevent evaporation, the cavity of the vial electrode can be sealed with a layer of mineral oil to make a closed system as described below. Notably, the use of bulk metal (rather than evaporated thin films) as the electrode structure leads to a robust and simple device that is readily cleaned prior to reuse. In contrast to studies using recessed electrodes, referred to above,[22−33] this method also has the advantage of not requiring the use of infrastructurally demanding equipment such as photolithography or screen-printing to fabricate devices suitable for the studies described below.

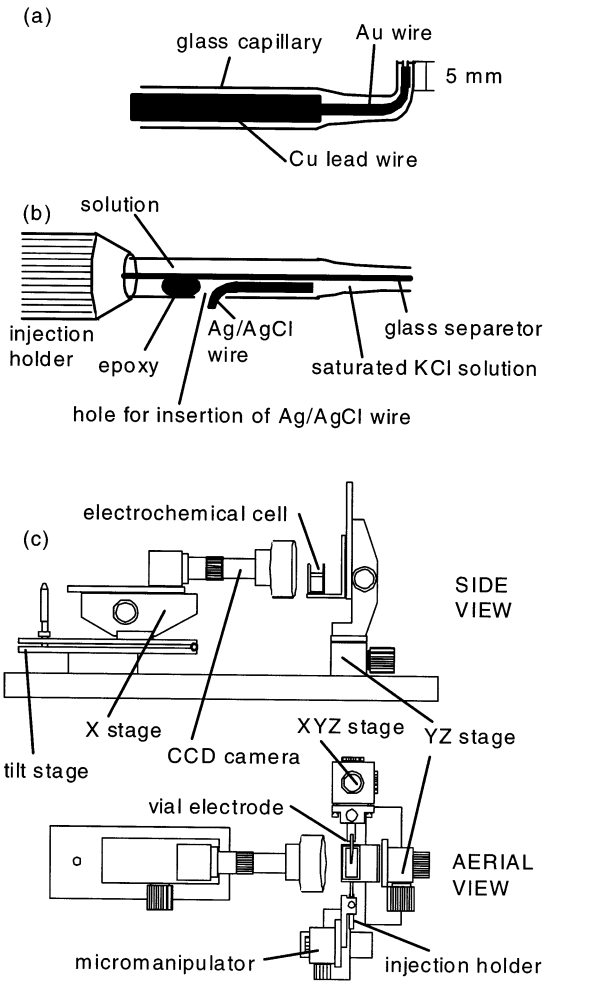

Figure 1. (a) Vial electrode, (b) injection capillary incorporating reference/counter electrodes, and (c) measurement system.

The electrochemical behavior of these vial electrodes was characterized, and the devices were subsequently used to measure metabolic flux from single plant cells. In this model biological system, an estimate was made of the size and character of the strong oxidative stress that occurs when the integrity of the cell membrane is challenged. The phenomenon of the production of reactive oxygen species, such as the superoxide anion, hydroxyl radicals, and hydrogen peroxide, has been described previously.[38,39] For example, a number of investigations have been undertaken using electron spin resonance[40,41] and fluorescence microscopy[42−44] and electrochemical analysis[5−7] of ensembles of cells. Notable previous electroanalytical investigations of these reactive species have included monitoring their release from both multicell ensembles[45] and single cells, the latter by physically

(29) Yi, C.; Gratzl, M. *Anal. Chem.* **1994**, *66*, 1976−1982.
(30) Yi, C.; Huang, D.; Gratzl, M. *Anal. Chem.* **1996**, *68*, 1580−1584.
(31) Briceno, G.; Change, H. Y.; Sun, X. D.; Schultz, P. G.; Xiang, X. D. *Science* **1995**, *270*, 273−275.
(32) Fritsch, I.; Henry, C. S. *J. Electrochem. Soc.* **1999**, *146*, 3367−3373.
(33) Fritsch, I.; Henry, C. S. *Anal. Chem.* **1999**, *71*, 550−556.
(34) Chan, T. K.; Luo, G.; Ewing, A. G. *Anal. Chem.* **1994**, *66*, 3031−3035.
(35) *Scanning Electrochemical Microscopy*; Bard, A. J., Mirkin, M. V., Eds.; Marcel Dekker: New York, 2001.
(36) Bard, A. J.; Fan, F.-R. F.; Kwak, J.; Lev, O. *Anal. Chem.* **1989**, *61*, 132−138.
(37) Engstrom, R. C.; Pharr, C. M. *Anal. Chem.* **1989**, *61*, 1099A−1104A.
(38) Halliwell, B.; Gutteridge, J. M. C. *Free Radicals in Biology and Medicine*, 3rd ed.; Oxford University Press: Oxford, U.K., 1999.
(39) Mallick, N.; Mohn, F. H. *J. Plant Physiol.* **2000**, *157*, 183−193.
(40) Ozawa, T., Tatsumi, K., Hori, T.-a., Eds. *Biodefence mechanisms against environmental stress*; Kodansha: Tokyo, 1998.
(41) Togashi, H.; Shinzawa, H.; Matsuo, T.; Takeda, Y.; Takahashi, T.; Aoyama, M.; Oikawa, K.; Kamada, H. *Free Radical Biol. Med.* **2000**, *28*, 846−853.
(42) Petrat, F.; de Groot, H.; Sustmann, R.; Rauen, U. *J. Biol. Chem.* **2002**, *383*, 489−502.
(43) Wei, T. T.; Zhang, C. Y.; Hou, J. W.; Chen, C.; Ma, H.; Chen, D. Y.; Xin, W. *J. Res. Chem. Intermed.* **2000**, *26*, 875−883.
(44) Juven, B. J.; Pierson, M. D. *J. Food Prot.* **1996**, *59*, 1233−1241.

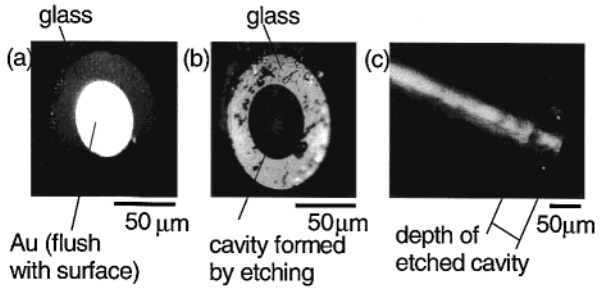

Figure 2. Optical microscope images of (a) the tip area of the gold microdisk electrode, together with (b) the face and (c) the side view of the vial electrode.

induced stress.[5−7] However, as stated previously, such measurements are, by their nature, spatially localized and therefore do not provide information on the total quantity of electroactive species released from the single cell. By confining the volume of solution around the cell, the method described here offers a simple means to detect the amount of electroactive species released during oxidative stress or exocytosis. As in other studies,[46,47] enzyme-linked electrochemical assays provide a convenient route to quantitatively determine metabolic flux of specific species from cells.

EXPERIMENTAL SECTION

Reagents. Potassium ferrocyanide, L-ascorbic acid (AA), ferrocenemethanol (FcOH), hydrogen peroxide (30%), horseradish peroxidase (HRP), catalase, ascorbate oxidase (AOx), sodium dodecyl sulfate (SDS), and mineral oil were purchased from Sigma and used without further purification. All the solutions were prepared from distilled and deionized water obtained from Aquarius GS-200 (Advantec) or Milli-Q Jr. (Millipore) systems.

Fabrication of Vial Electrodes. Picoliter-sized vial electrodes (Figure 1a) were fabricated from microdisk electrodes constructed as described in previous publications.[48,49] The microelectrodes comprising embedded gold wire (radius 25 μm) were first heated 5 mm from the top of the tip using a platinum wire heating loop, and the softened glass formed a bend of ~90° in the glass capillary. The gold tip was etched electrochemically (300 Hz, ac voltage with 5−10 V peak-to-peak) for 10−20 min in a saturated aqueous solution of $NaNO_3$. Controlling the etching time and intensity of voltage varied the depth of the cavity (Figure 2).

Fabrication of an Injection Capillary. The composite reference/counter electrode was constructed within an injection capillary; see Figure 1b. A θ-type (conjoined double-capillary) glass tube (World Precision Instruments, Tokyo, Japan) was pulled using a capillary puller (model PD-5, Narishige, Tokyo, Japan) to make a capillary with two openings, each of 0.05-μm radius. An aperture was made in one of the two joined capillaries, a Ag/AgCl wire was inserted, and the tube was filled with a saturated KCl solution. The Ag/AgCl wire was held in place using epoxy and was used as a reference/counter electrode. This composite electrode assembly was connected to a microinjector (IM300, Narishige), thereby allowing the nonreference electrode opening to be used to inject precise picoliter-scale quantities of solution into the analytical chamber.

Measurement System. All measurements were performed using an inverted microscope (MSL2PL, Meiji Techno, Saitama, Japan), a multipotentiostat (HA-1512μM8, Hokuto Denko, Tokyo, Japan), a CCD video camera (STC-630A, Kenko, Tokyo, Japan), a micromanipulator (MM-200, Narishige), a tilt stage (TS-201, Chuo Precision Industrial, Tokyo, Japan), an X stage (LS-612, Chuo Precision Industrial), a YZ stage (LM-612, Chuo Precision Industrial), and an XYZ stage (C7214-9015, Suruga Seiki Co., Ltd., Shizuoka, Japan) (Figure 1c). The precise position of the vial electrode and microelectrode tip was determined by imaging both the chamber and the injection system with a CCD video camera. Control of electrode potential and data acquisition were performed with a notebook computer equipped with a 16-bit AD/DA board (AZI-3506, Interface, Hiroshima, Japan). The analytical chamber−electrode assembly was mounted on the XYZ stage, and the composite reference/counter electrode and injection port was attached to separate micromanipulators. The chamber and the injection port were positioned with respect to each other, such that the tip of the composite reference/counter electrode and injection port assembly was inserted into the opening of the vial electrode. All the measurements were performed at 25 °C in a Faraday cage.

Preparation of Protoplasts. Protoplasts were made from marine alga *Bryopsis plumosa* by the method reported previously[50] in synthetic artificial seawater containing 480.2 mM NaCl, 2.3 mM $NaHCO_3$, 11.1 mM $CaCl_2$, and 83.3 mM $MgCl_2$ (pH 7.6). All the amperometric measurements were started between 20 and 30 min after the protoplast preparation was complete. For electrochemical analysis of a single protoplast, the vial electrode was "primed" in a beaker containing artificial seawater. A single cell (20-μm radius) was collected using a small capillary and was inserted into the analytical chamber. The tip of the composite reference/counter microelectrode assembly was positioned in the cavity of the vial electrode. Finally, mineral oil (~10 pL) was carefully added to the surface of the seawater and the beaker lowered to leave the cavity filled with the seawater. Evaporation at the air interface was prevented by the mineral oil layer, as described previously.[23]

RESULTS AND DISCUSSION

Electrode Structure. Figure 2 shows optical microscope images for tip areas of the gold microdisk electrode (a) and subnanoliter-sized vial electrode (b and c). The optical microscope image of the microdisk electrode indicates that the fine gold wire is encased in the glass capillary and exposed as a disk shape with a radius of ~25 μm. The images of the vial electrode fabricated with electrochemical etching indicate that the gold wire dissolves to give a small vial of radius 25 μm and depth 50 μm (geometric volume ~100 pL).

Electrochemical Characterization by Cyclic Voltammetry. Prior to their use in analyzing the total quantities of electrochemically active cellular material released during oxidative stress, a

(45) Manning, P.; McNeil, C. J.; Cooper, J. M.; Hillhouse, E. W. *Free Radicals* **1998**, *24*, 1304−1309.
(46) Rishpon, J.; Gezundhajt, Y.; Soussan, L.; Rosenmargalit, I.; Hadas, E. *ACS Sym. Ser.* **1992**, *511*, 59−72.
(47) Darder, M.; Casero, E.; Pariente, F.; Lorenzo, E. *Anal. Chem.* **2000**, *72*, 3784−3792.
(48) Shiku, H.; Takeda, T.; Yamada, H.; Matsue, T.; Uchida, I. *Anal. Chem.* **1995**, *67*, 312−317.
(49) Yasukawa, T.; Uchida, I.; Matsue, T. *Biochim. Biophys. Acta* **1998**, *1369*, 152−158.
(50) Tatewaki, M.; Nagata, K. *J. Phycol.* **1970**, *4*, 401−403.

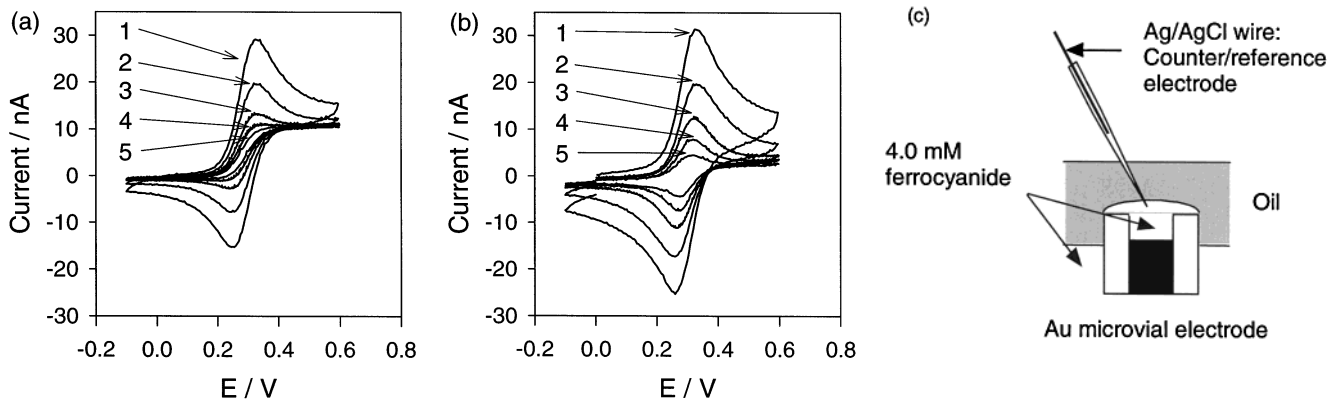

Figure 3. Cyclic voltammograms of 4.0 mM ferrocyanide at various scan rates ((1) 100, (2) 50, (3) 20, (4) 10, and (5) 5 mV/s) for a vial electrode immersed in (a) the bulk solution and (b) when sealed by a thin film of oil. (c) Schematic of experimental arrangement.

study was made of the electrochemical response of the vial electrodes to species similar to those involved in the cell metabolite assays described below, namely, ascorbic acid, H_2O_2, and the model redox ion ferrocyanide. For example, cyclic voltammetric characterization was performed using either a 4.0 mM ferrocyanide or a 1.0 mM ascorbic acid solution. Figure 3 shows cyclic voltammograms at a number of scan rates ((1) 100, (2) 50, (3) 20, (4) 10, and (5) 5 mV/s) for a vial electrode immersed in (a) the bulk solution and (b) when sealed by the oil (as illustrated in Figure 3c). Cyclic voltammograms of the vial electrode in the bulk solution show both oxidation and reduction peaks for the ferrocyanide/ferricyanide species, when the scan rate, v, is more than 20 mV/s. The characteristic form of these peaks are a consequence of the fact that the solution sampled on this time scale is wholly contained within the vial and thus only *linear* diffusion to the vial electrode occurs. At lower scan rates (i.e., $v < 10$ mV/s), the cyclic voltammograms show a steady-state current at potentials above 0.4 V. In a simple model for this response, the mass transfer to the electrode surface is theoretically treated as simple linear diffusion (normal direction to the planar electrode). If we assume that the concentration of electroactive species outside the vial is maintained at that of the bulk solution and that the concentration gradient within the vial is linear, the steady-state current is given by an expression obtained from Fick's Ist Law. This predicts a steady-state current of 11.8 nA which is slightly larger than that measured, 10.5 nA (the difference possibly arising as a consequence of the depletion layer extending slightly into the bulk solution).

At scan rates in excess of 20 mV/s, the voltammograms for the sealed analytical chamber (Figure 3b) similarly show oxidation peaks that are of a size comparable to those obtained using unsealed chambers; however, the reduction peaks are larger than those measured in unsealed chambers because ferricyanide generated by the oxidation reaction cannot escape to bulk solution. In contrast to the observed response of unsealed chambers, as the scan rate is lowered, the oxidation peaks persist in the voltammograms and do not degenerate to plateaus. The appearance of redox peaks in the slow scan rate voltammograms using a sealed microcavity is a consequence of the lack of mass transport from a bulk solution and is similar to voltammetry characteristic of thin-layer cells.[51]

Figure 4 shows cyclic voltammograms of a vial electrode in 1.0 mM ascorbic acid when immersed in the bulk solution (a) and when sealed by the oil (b), at various scan rates ((1) 100, (2) 50, (3) 20, (4) 10, and (5) 5 mV/s). The cyclic voltammograms in the bulk solution show oxidation peaks and, as expected, show no reduction current, when $v > 20$ mV/s due to the electrochemically irreversible nature of the oxidation process. As with the model ferro/ferricyanide system (Figure 3a), when $v \leq 10$ mV/s, the voltammograms show plateaulike steady-state currents

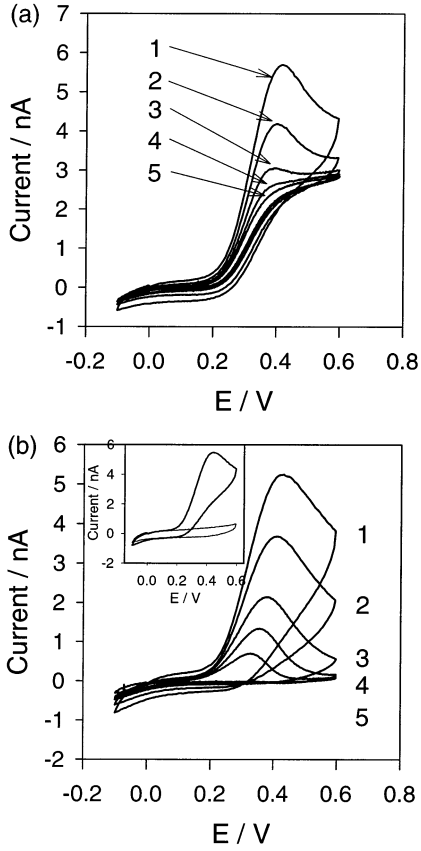

Figure 4. Cyclic voltammograms of a vial electrode in 1.0 mM AA (a) when immersed in the bulk solution and (b) when sealed by a thin film of oil, at various scan rates ((1) 100, (2) 50, (3) 20, (4) 10, and (5) 5 mV/s). Inset: cyclic voltammograms (scan rate, 100 mV/s) for 1.0 mM AA of the second scans in the sealed vial.

(51) Bard, A. J.; Faulkner, L. R. *Electrochemical Methods: Fundamentals and Applications*; John Wiley: New York, 1980; pp 406−413.

Scheme 1. Detection of Ascorbate[a]

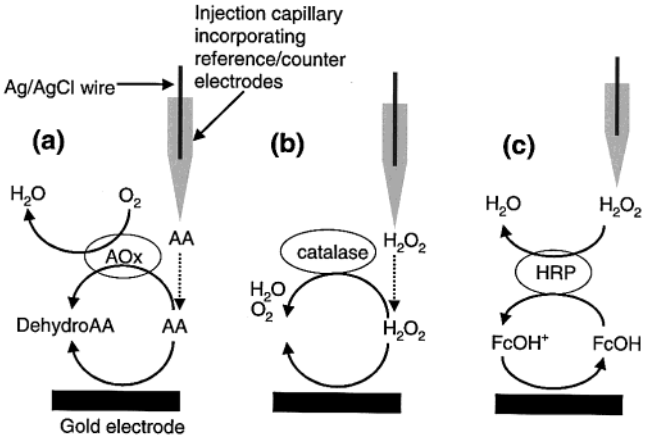

[a] (a) Detection of ascorbate either directly through electrochemical oxidation at a gold electrode, or indirectly, in the presence of ascorbate oxidase, by the decrease in dioxygen reduction current (dotted line indicates ascorbate being injected from the capillary tip). (b) Detection of H_2O_2 by direct electrochemical oxidation. (c) Detection of H_2O_2 by reduction of $FcOH^+$ species that mediate the peroxidase-catalyzed reaction.

for the oxidation of ascorbic acid. Again, when the oil film-sealed chambers are used, a peak in the oxidation current is seen at all scan rates. For these latter, sealed chambers, oxidation currents decrease toward zero at sufficiently large anodic voltages when $v \leq 10$ mV/s. Again, these results are similar to those obtained in thin-layer voltammetry studies.[51]

The magnitude of the peak current for ascorbate oxidation is proportional to the scan rate (data not shown). This suggests that the ascorbate in the chamber was completely consumed by the electrochemical reaction in the time taken for the anodic potential scan. The quantity of ascorbate in the chamber estimated by integration of the background-corrected current (at $v = 5$ mV/s) was found to be ~125 fmol ($n = 5$), slightly greater than that estimated from simple geometric calculations of the vial volume. This discrepancy between the calculated (geometric) volume and the actual volume is likely to be due to the visible curvature of the meniscus formed at the water/oil interface.

Due to the irreversible nature of the ascorbate oxidation, between successive voltammograms performed on the sealed chambers, the solution within the vial was replenished by reimmersing the vial into the bulk solution. Notably, the inset of Figure 4 shows the first and second cyclic voltammograms ($v =$ 100 mV/s) for 1.0 mM ascorbate when the vial solution is not refreshed. This inset shows that an oxidation current for ascorbate is observed during the first CV, but negligible current is observed during the second CV. This indicates that there is no residual ascorbate or other oxidizable material in the vial after completion of the first oxidation scan (the oxidized ascorbate having undergone rapid chemical degradation to electroinactive species).

Amperometric Characterization. To experimentally simulate the electrochemical responses that might be expected when a protoplast in the vial is subjected to stress, a series of amperometric assay experiments were performed. Scheme 1 illustrates the use of the gold vial electrode to assay ascorbate or hydrogen peroxide either by direct electron transfer from these species or, when an enzyme is present, by measurements of appropriate enzyme mediators (dioxygen or ferrocenemethanol).

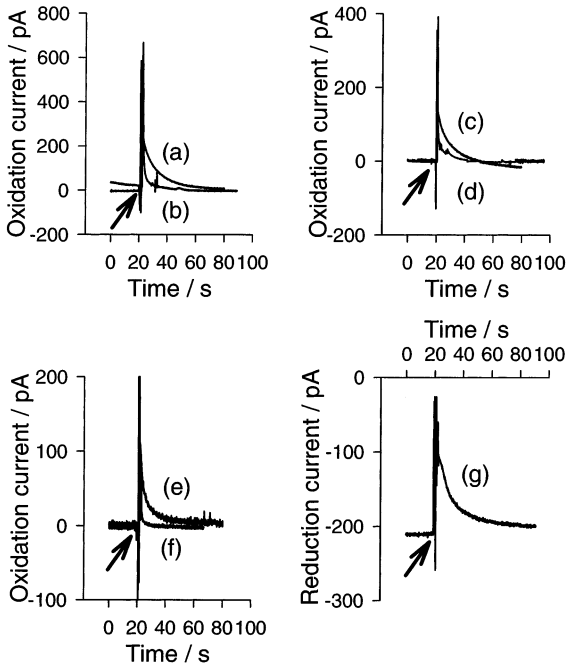

Figure 5. Amperometric response following AA injection into an oil-sealed microvial electrode. The following AA/artificial seawater solutions were injected at the point indicated by an arrow: (a) 5.0 mM AA, (b) 5.0 mM AA (vial contained 205 units/mL AOx), (c) 2.0 mM AA, (d) 2.0 mM AA (vial contained 205 units/mL AOx), (e) 1.0 mM AA, (f) 1.0 mM AA (vial contained 205 units/mL AOx), and (g) 2.0 mM AA (vial contained 205 units/mL AOx). Volume of injected solution in the vial was calculated from these results and found to be ~2.9 pL. The electrode potential was held at 0.60 (a−f) and −0.50 V (g).

Thus, Figure 5 shows the responses of the vial electrode after various concentrations of ascorbate were injected both in the absence and in the presence of the enzyme AOx. The electrode potential was held at either 0.60 V to monitor the oxidation of ascorbate (Figure 5a−f) or at −0.50 V to observe the reduction of oxygen (Figure 5g). Immediately after injection of ascorbic acid, the (oxidation) current increased and returned the original level (zero) after 30−60 s (Figure 5a, c, and e). The time scale of this current transient is consistent with the assumption that all the ascorbate within the chamber is completely consumed by an electrochemical reaction. Since the products formed at the counter electrode are effectively in a separate compartment, the quantities of injected ascorbate can be calculated by integration of the current. For injections from 5, 2, and 1 mM ascorbate solutions, the quantity of substrate in the chamber was estimated as 13.5, 5.8, and 3.0 fmol, respectively. Importantly, the quantity of charge for the electrochemical oxidation reaction was found to be proportional to the concentration of ascorbate injected, indicating that the same volume of solution was injected each time.

When the chamber solution contained 205 units mL^{-1} AOx prior to ascorbate injection, the current due to the electrochemical oxidation of ascorbate decreased (Figure 5b, d, and f). Integration of the current at the working microelectrode during the electrochemical oxidation showed that the charge transferred had decreased to 42.6 ± 6.3% ($n = 15$) of that in the absence AOx. The response characteristics to ascorbate are summarized in Table 1.

Table 1. Response Characteristics to AA and H_2O_2 When They Were Injected in the Vial Electrode

concn (mM)	enzyme[a]	electrode potential (V)	transferred charge (pC)	quantity (fmol)	injected vol (pL)	proportion of AA or H_2O_2[b] (%)
			Injected Compound: AA			
5	none	0.60	2610 ± 421	13.5 ± 2.2	2.7 ± 0.4	
2		0.60	1123 ± 110	5.8 ± 0.6	2.9 ± 0.3	
1		0.60	595 ± 96	3.0 ± 0.5	3.0 ± 0.5	
5	AOx	0.60	1115 ± 155	5.8 ± 0.8		43.0 ± 5.9
2		0.60	463 ± 52	2.4 ± 0.3		41.4 ± 5.1
1		0.60	251 ± 24	1.3 ± 0.2		43.3 ± 4.0
2		−0.50	914 ± 240[c]	4.7 ± 1.2		
			Injected Compound: H_2O_2			
5	none	0.60	4763 ± 439	26.4 ± 4.0	5.0 ± 0.4	
2		0.60	1978 ± 256	10.3 ± 1.4	5.1 ± 0.7	
1		0.60	994 ± 161	5.1 ± 0.8	5.1 ± 0.8	
5	catalase	0.60	1679 ± 430	8.7 ± 2.2		33.0 ± 8.3
2		0.60	713 ± 175	3.7 ± 0.9		35.9 ± 8.8
1		0.60	372 ± 46	2.0 ± 0.3		39.2 ± 4.5
2	HRP	0.05	1835 ± 217	9.5 ± 1.1		

[a] Enzyme injected into the vial. [b] Estimated by comparing the charge passed in the presence and absence of the appropriate enzyme. [c] Calculated by measuring the decrease in current due to the reduction of oxygen as a result of oxygen consumption in the AOx-catalyzed reaction.

The change in the magnitude of the oxygen reduction current was also measured following ascorbate injection into a vial containing an AOx solution (Figure 5g). Under quiescent conditions, there is a steady-state reduction current of ~210 pA (the steady-state current was limited by the diffusion of oxygen through the mineral oil layer). It is also notable that, when ascorbate was injected in the vial containing AOx, the magnitude of the reduction current decreased. These results suggest that the injected ascorbate was oxidized to dehydroascorbic acid by the AOx enzyme reaction, resulting in the consumption of oxygen (and the subsequent reduced availability for electroreduction).

The results presented above establish that it is possible to inject a predetermined quantity of ascorbate into a picoliter-volume chamber and that the ascorbate is completely consumed by an electrochemical or enzyme reaction in an appropriate time scale for single-cell analysis. It is noted that there is competition between direct electrode oxidation and enzymatic oxidation (the rate of the AOx-catalyzed reaction combined with solution mixing limitations is not fast enough to exclusively oxidize all of the substrate).

Experiments similar to those above were carried out to determine the characteristic electrochemical responses of the vial electrode to H_2O_2-containing solutions. Figure 6 shows amperometric responses of a microelectrode to the injection of aliquots of different concentrations of H_2O_2. The electrode potential was held at 0.60 V for direct detection of H_2O_2 through oxidation (Figure 6a−f). Experiments analogous to those in the presence of AOx (described above) were performed using vial solutions containing 185 units mL^{-1} catalase to consume the injected H_2O_2. The response characteristics of the microelectrode following H_2O_2 injection are summarized in Table 1.

A third, alternative electrochemical assay appropriate to the cell measurements described below was characterized in the vial electrode system. This involves the catalysis of H_2O_2 by the enzyme HRP in the presence of FcOH as a mediator. When HRP and FcOH are injected in the vial, the electrode potential is held at 0.05 V to reduce the oxidized form of FcOH (Figure 6g). Injection of 2.0 mM H_2O_2 into a vial containing 120 units mL^{-1} HRP and 1.0 mM FcOH results in a readily measurable reduction current transient. The quantity of injected H_2O_2 was calculated from the quantity of FcOH reduced at the microelectrode and was found to be 9.5 fmol when 2.0 mM H_2O_2 was injected. This quantity is consistent with that calculated using volume estimates derived from the oxidation current following H_2O_2 injection in the absence of an enzyme. As with the ascorbate measurements, these results establish that precise quantities of H_2O_2 solution can be

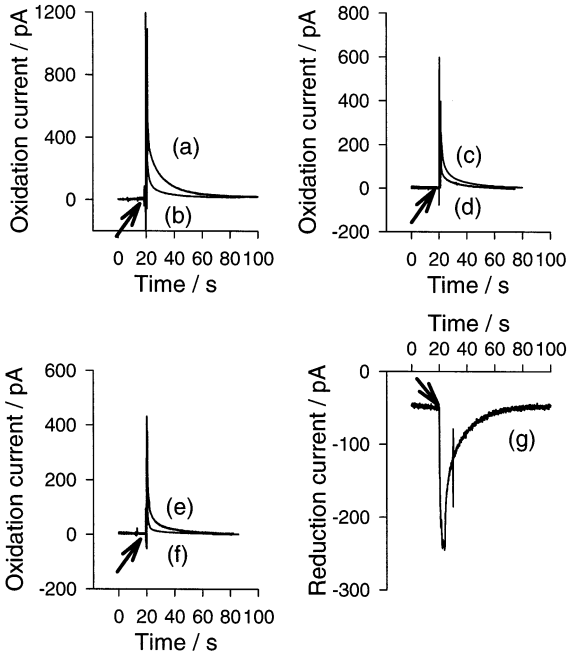

Figure 6. Amperometric oxidation of H_2O_2 by oil-sealed microvial electrode. The following H_2O_2/artificial seawater solutions were injected at the point indicated by an arrow: (a) 5.0 mM H_2O_2, (b) 5.0 mM H_2O_2 (vial contained 185 units/mL catalase), (c) 2.0 mM H_2O_2, (d) 2.0 mM H_2O_2 (vial contained 185 units/mL catalase), (e) 1.0 mM H_2O_2, (f) 1.0 mM H_2O_2 (vial contained 185 units/mL catalase), and (g) 2.0 mM H_2O_2 (vial contained 120 units/mL HRP and 1.0 mM FcOH). Volume of injected solution in the vial was calculated from these results and found to be ~5.1 pL. The electrode potential was held at 0.60 (a−f) and 0.05 V (g).

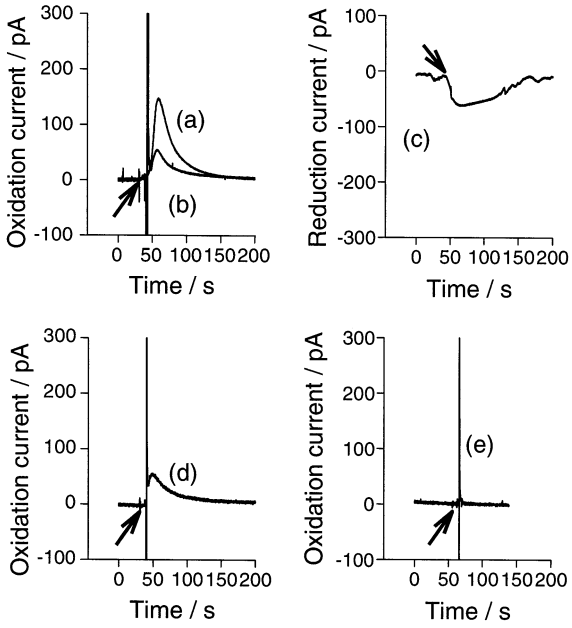

Figure 7. Electroactive species released from single cells (20-μm radius) destroyed by injection of 10 mM SDS in to the vial. 10 mM SDS/artificial seawater solutions were injected at the point indicated by an arrow. Prior to injection, the vials contained (a) enzyme-free solution, (b) 185 units/mL catalase solution, (c) 120 units/mL HRP and 1.0 mM FcOH (reduced form), (d) 185 units/mL catalase and 205 units/mL AOx, and (e) artificial seawater. The electrode potential was held at 0.60 (a−d) and 0.05 V (e).

injected into a vial and that the H_2O_2 is completely consumed by either an electrochemical or an appropriate enzyme reaction.

Single-Cell Measurements. A single protoplast was placed into the chamber, and the surface sealed with the mineral oil, as before. Injection of 10 mM SDS into the solution around the cell compromises the integrity of the cell membrane, and variations of anodic current were subsequently measured using amperometry at 0.60 V (Figure 7). It was observed that the oxidation current started to increase a few seconds after injection of SDS. The peak in the oxidation current occurred ∼20 s after addition of SDS, followed by a gradual decay in the current toward zero after 120 s (Figure 7a). This current increase corresponds to the oxidation of electroactive species released following the oxidative burst that occurs on injection of the SDS. Appropriate controls were carried out in the presence of SDS and absence of cells to establish that negligible background currents resulted from this injection procedure (data not shown).

The inclusion of AOx and catalase (both separately and together) in the solution around the cell was used to investigate the nature of the products released from the cell during its oxidative burst and its destruction. Figure 7b shows the change in the oxidation current as the living cell, surrounded by a solution containing 185 units mL^{-1} catalase, is compromised by the addition of SDS. Shortly after SDS addition, the current due to oxidation of electroactive species increased as the cell membrane dissolved. The magnitude of the oxidation current was consistently smaller than in similar experiments performed in the absence of catalase, suggesting that the oxidative burst (involving superoxide release) involves the generation of H_2O_2. Using the same assumptions that were made in the amperometric characterization above, the difference in oxidative charge in Figure 7a and b corresponds to the release of 22.2 ± 8.7 fmol (n = 8) of H_2O_2 during cell destruction. This value is ∼85% of the whole electrochemical oxidation response obtained during cell death. The charge transferred due to oxidation of electroactive species released by the cell destruction is summarized in Table 2.

Table 2. Charge Transferred due to Electroactive Species Released during Cell Destruction

enzyme included in the vial electrode	charge transferred (nC)
none	5.0 ± 0.5
catalase	2.2 ± 0.6
AOx	5.2 ± 0.7
catalase and AOx	2.0 ± 0.6

Experiments were also performed in which the solution around the cell contained 120 units mL^{-1} HRP and 1.0 mM FcOH. Again, the cell was destroyed in the vial by injecting 10 mM SDS and the oxidized FcOH was detected by the vial electrode at 0.05 V (Figure 7c). This result also confirmed that H_2O_2 is released from the cell and reduced by the HRP enzyme reaction mediated by FcOH oxidation. The quantities of H_2O_2 generated from the cell were calculated from the charge corresponding to $FcOH^+$ reduction and were found to be ∼18.1 fmol. Although this is consistent with that determined above, the slightly lower value may be due to other metabolites in the cell, rather than FcOH, acting as a mediator for HRP.

Taken together, the results in the presence of catalase or HRP suggest that the oxidative burst in cell destruction involves the simultaneous release of a variety of electroactive species with most of the reactive oxygen species generated by oxidative stress being detected as H_2O_2 outside of the cell. When similar SDS-induced stress experiments were performed in the presence of AOx and catalase, a decrease in the oxidation response was not observed (Figure 7d, Table 2), indicating that ascorbate is not released outside of the cell during oxidative stress (it is, however, possible that, as an antioxidant, it is converted to dehydroascorbic acid by reactive oxygen species generated during the oxidative burst). For comparative purposes, the lack of electrochemical response on injection of SDS-free seawater is also shown (Figure 7e). Thus, it is likely that the excess oxidation charge above the 85% attributed to H_2O_2 is not associated with ascorbate oxidation. The possibility of the remaining oxidizable material being due to species such as NO could be investigated by the use of vial electrodes coated with a suitable sensing polymer film (such as a manganese porphyrin system linked to poly(pyrrole)[52]). In such experiments, as above, catalase would be used to remove the H_2O_2 component of the solution and thus eliminate the electrochemical currents due to H_2O_2 oxidation.

CONCLUSION

The microelectrode described here is electrochemically characterized, and the results are found to correlate well with theoretical calculations. Measurements on a single cell in a vial demonstrate that the system is suitable to investigate the whole quantities of important intracellular substances. The released electroactive species can be monitored electrochemically and,

(52) Diab, N.; Schuhmann, W. *Electrochim. Acta* **2001**, *47* (1−2), 265−273.

through the inclusion of various enzymes in the vial solution, a proportion of this current ascribed to certain species. Importantly, it is found that similar quantities of H_2O_2 are detected during oxidative stress measurements when two different enzyme-based assays are used.

When these measurements are performed, there is the potential that an electrode coming into contact with the cell could influence the cell's response. However, similar quantities of H_2O_2 were determined when different assays were used in which the electrode reaction was either oxidizing (0.60 V vs Ag/AgCl) or reducing (0.05 V) prior to the lysis of the membrane with SDS, suggesting that the electrode potential does not unduly perturb or stress these cells.

This general methodology may be applicable to the study of species excreted during single-cell metabolism using enzyme-linked assays. For instance, in recent work,[53] reduction in the activity of BY2 cells was electrochemically investigated when cells were treated with several stress compounds such as elicitors, plant hormones, and metabolic and electron transport inhibitors. In the future, one application of the system described here could be the investigation of processes such as these at the single-cell level.

(53) Kinpara, T.; Murakami, Y.; Yokoyama, K.; Tamiya, E. *Electroanalysis* **2001**, *13*, 451−456.

ACKNOWLEDGMENT

This work was partly supported by Grants-in-Aid for Scientific Research on Priority Areas (Single-Cell Molecular Technology, 11227201) and for Scientific Research B (11450323) from the Ministry of Education, Science and Culture, Japan. T.Y. acknowledges a research fellowship from the Royal Society UK, for travel to Scotland.

Received for review June 7, 2002. Accepted July 23, 2002.

AC025836U